Intracellular Proton-Transfer Mutants in a CLC Cl^-/H^+ Exchanger

Hyun-Ho Lim and Christopher Miller

Department of Biochemistry, Howard Hughes Medical Institute, Brandeis University, Waltham, MA 02454

CLC-ec1, a bacterial homologue of the CLC family's transporter subclass, catalyzes transmembrane exchange of Cl^- and H^+. Mutational analysis based on the known structure reveals several key residues required for coupling H^+ to the stoichiometric countermovement of Cl^-. E148 (Glu_{ex}) transfers protons between extracellular water and the protein interior, and E203 (Glu_{in}) is thought to function analogously on the intracellular face of the protein. Mutation of either residue eliminates H^+ transport while preserving Cl^- transport. We tested the role of Glu_{in} by examining structural and functional properties of mutants at this position. Certain dissociable side chains (E, D, H, K, R, but not C and Y) retain H^+/Cl^- exchanger activity to varying degrees, while other mutations (V, I, or C) abolish H^+ coupling and severely inhibit Cl^- flux. Transporters substituted with other nonprotonatable side chains (Q, S, and A) show highly impaired H^+ transport with substantial Cl^- transport. Influence on H^+ transport of side chain length and acidity was assessed using a single-cysteine mutant to introduce non-natural side chains. Crystal structures of both coupled (E203H) and uncoupled (E203V) mutants are similar to wild type. The results support the idea that Glu_{in} is the internal proton-transfer residue that delivers protons from intracellular solution to the protein interior, where they couple to Cl^- movements to bring about Cl^-/H^+ exchange.

The Journal of General Physiology

INTRODUCTION

Membrane proteins of the ubiquitous CLC family operate in varied physiological contexts, calling for transmembrane movement of inorganic anions (Jentsch, 2008). These proteins segregate into two distinct mechanistic subtypes: Cl^--specific channels and proton-coupled Cl^- (or, in plants, NO_3^-) exchangers (Zifarelli and Pusch, 2007). The channels have been studied electrophysiologically for many years, but the exchange transporters, recently recognized, are understood only in fuzzy mechanistic outline. Built as homodimers in which each subunit operates as a full-fledged exchanger (Nguitragool and Miller, 2007; Zdebik et al., 2008), these proteins swap substrate ions across the membrane in opposite directions with a stoichiometry of two Cl^- ions per H^+ (Accardi and Miller, 2004; DeAngeli et al., 2006; Nguitragool and Miller, 2006; Graves et al., 2008; Miller and Nguitragool, 2009). The x-ray crystal structure of CLC-ec1 from *Escherichia coli*, the only structurally known CLC, provides a view of the physical pathways by which Cl^- and H^+ move through proteins of this family (Dutzler et al., 2003; Miller, 2006). A mechanistic scheme for how these movements are coordinated has recently been proposed (Miller and Nguitragool, 2009).

Coupled Cl^-/H^+ transport uses two strictly conserved glutamates near the protein's extracellular or intracellular surfaces to transfer protons between the proximate aqueous solutions and the protein interior (E148 and E203 in CLC-ec1, denoted Glu_{ex} and Glu_{in}, respectively). Substituting either of these residues with nonprotonatable side chains eliminates H^+ but retains Cl^- movement (Accardi and Miller, 2004; Accardi et al., 2005; Picollo and Pusch, 2005; Scheel et al., 2005; Jayaram et al., 2008; Zdebik et al., 2008). The proton-transfer function of Glu_{ex} is well established experimentally (Dutzler et al., 2003; Accardi and Miller, 2004): the side chain acts as a "gate" that blocks off the extracellular end of the Cl^- pathway when deprotonated and swings away upon protonation to open this pathway to the outside. But the role of Glu_{in} on the intracellular side is not so clear. It is known that this is the only internally facing carboxyl group that when mutated away abolishes H^+ transport (Accardi et al., 2005), and a recent molecular dynamics simulation suggests that a side chain rotation of Glu_{in} is required for transferring H^+ into the proton pathway (Voth, G., personal communication); but no such structural rearrangement of Glu_{in} has been observed crystallographically. Further experimental scrutiny is therefore needed to test the idea that this residue is an intracellular H^+ transfer catalyst. Now, by examining an expanded panel of mutations at Glu_{in}, we show that Cl^-/H^+ exchange is supported only by protonatable side chains, both acidic and basic, and that non-dissociable side chains produce uncoupled Cl^- transporters with a wide range of absolute rates. These

Correspondence to Christopher Miller: cmiller@brandeis.edu

Abbreviations used in this paper: DM, decylmaltoside; FCCP, p-trifluoromethoxyphenyl hydrazone; FIAA, fluoro-iodoacetic acid; IAA, iodoacetic acid; Vln, valinomycin; WB, wash buffer; WT, wild-type.

The Rockefeller University Press $30.00
J. Gen. Physiol. Vol. 133 No. 2 131–138
www.jgp.org/cgi/doi/10.1085/jgp.200810112

results agree in outline, but not in all details, with similar experiments on mammalian CLC exchangers (Zdebik et al., 2008), and they corroborate the proposal (Accardi et al., 2005) that Glu_{in} shuttles protons between the intracellular solution and the still unknown internal workings of the exchanger.

MATERIALS AND METHODS

Biochemical Procedures

Chemicals were of the highest grade available. Fluoro-iodoacetic acid (FIAA) was obtained from American Custom Chemicals, methanethiosulfonate compounds were from Toronto Research Chemicals, detergents were from Anatrace, and phospholipids were from Avanti Polar Lipids, Inc. Protein purification and reconstitution procedures were, with minor modifications, as described previously (Accardi et al., 2004; Walden et al., 2007). In brief, mutants of CLC-ec1 (GenBank accession no. P37019), His_6 tagged at the C terminus, were constructed by PCR mutagenesis, and the full coding sequence was confirmed. These were expressed in *E. coli*, extracted in decylmaltoside (DM), and partially purified on Co-affinity beads (BD) by sequentially washing with 10–20 column volumes of wash buffer (WB; 100 mM NaCl, 20 mM tris-Cl, and 5 mM DM, pH 7.5), 10 vol of WB containing 20 mM imidazole, 10 vol of high salt WB (1 M NaCl, 20 mM tris-Cl, and 5 mM DM, pH 7.5), and 10 vol of WB. Protein was eluted with WB containing 400 mM imidazole, and the His tag was removed by a 1-h digestion with lysine endoproteinase C (0.05 U/mg protein; Roche). Protein was further purified by anion-exchange chromatography (Poros HQ; Applied Biosystems) for planar lipid bilayer experiments or gel filtration (Superdex 200) for liposome flux assays and for structure determination. Purified protein was reconstituted at various protein densities (0.2–50 µg/mg lipid) into liposomes formed by detergent dialysis from *E. coli* phospholipids and stored at 20 mg lipid/ml at −80°C in aliquots. All mutants expressed well (1–3 mg/L culture) and ran as homodimers on gel filtration chromatography.

For introducing non-natural side chains into the Glu_{in} position, a single-cysteine mutant, E203C, on a cysteine-free background (C84A/C302A/C347S) was used (Nguitragool and Miller, 2007). Various electrophilic reagents were reacted at pH 8.0 with this protein to form the desired side chain adducts: iodoacetic acid (IAA), FIAA, 2-carboxylethyl methanethiosulfonate, and 2-sulfonatoethyl methanethiosulfonate. Reactions were monitored quantitatively with the Ellman reagent, as described for this protein (Nguitragool and Miller, 2007). Protein samples were passed through Superdex 200 equilibrated with 50 mM NaCl, 50 mM NaP_i, and 5 mM DM, pH 8.0, and four shots of 1 mM MTS reagent was added at 15-min intervals. Reactions with 100 mM IAA or FIAA were run for 20 or 32 h, respectively. Reactions were terminated by gel filtration in 100 mM tris-Cl, 3 mM EDTA, and 5 mM DM, pH 8.0. Table S1, available at http://www.jgp.org/cgi/content/full/jgp.200810112/DC1, reports details of these cysteine-modification reactions.

H^+ Pumping and Cl^- Flux Assays

Cl^- gradient-driven H^+ pumping and passive Cl^- efflux assays were performed as described previously (Nguitragool and Miller, 2007; Walden et al., 2007; Jayaram et al., 2008), at pH 4–5, where CLC-ec1 is maximally active. Proton pumping used liposomes with high protein density (5.0 µg protein/mg lipid) loaded with 300 mM KCl and 40 mM citrate, pH 5.0. After thawing, liposomes were extruded with a 0.4-µm filter; just before each run, a 100-µl liposome sample was centrifuged through a 1.5-ml G-50 column equilibrated in pump buffer (290 mM K-isethionate, 10 mM KCl, and 2 mM glutamate, pH 5.2) to establish a Cl^- gradient. The liposomes were added to 1.8 ml of pump buffer in a stirred cell with pH continuously monitored with a glass electrode, and H^+ pumping was triggered by the addition of 0.5 µg/ml valinomycin (Vln). After ∼30 s, the pH gradient was collapsed with 0.5 µg/ml p-trifluoromethoxyphenyl hydrazone (FCCP).

For the Cl^- efflux assay, proteins were reconstituted at a low density (0.2 µg protein/mg lipid) for fast transporters or a high density (5 µg/mg) for slow mutants. Extruded liposomes were loaded with 300 mM KCl and 25 mM citrate, pH 4.5, for measuring turnover rates or with 300 mM KCl, 20 mM citrate, 10 mM MES, and 20 mM HEPES-NaOH, pH 4.0–7.5, for pH-dependent Cl^- transport assay, and spun in 100-µl samples through G-50 columns equilibrated in dump buffer (300 mM K-isethionate, 1 mM KCl, buffered as above). A sample was added to 1.8 ml of dump buffer in a stirred cell at 25°C monitored with a Cl^- electrode. Cl^- efflux was initiated by Vln and FCCP (0.5 µg/ml each), and at the end of the run, total trapped Cl^- was determined by disrupting liposomes with 50 mM β-octylglucoside. Transport turnover rate was calculated by the initial velocity method (Walden et al., 2007), using a 75-µM Cl^- addition to calibrate each experiment.

Electrical Recording in Planar Lipid Bilayers

Ionic currents mediated by CLC-ec1 were recorded as described in detail (Accardi et al., 2004). Recordings were made with either a 3-unit pH gradient (pH 4.0/7.0) at symmetrical 300 mM KCl or a 10-fold KCl gradient (300/30 mM) at symmetrical pH 4.0, buffered with 15 mM citrate-phosphate KOH. Families of 1-s voltage pulses from −100 to +100 mV in 10-mV increments were applied from a holding potential of zero voltage. Current signals were low-pass filtered at 1 kHz and digitized at 10 kHz using an Axopatch 200 amplifier and pClamp software.

X-ray Crystallography

Two mutants, E203V and E203H, in complex with a F_{AB} fragment were crystallized at 20°C in 100–150 mM NaBr (Lobet and Dutzler, 2005), harvested after 1–8 wk, and frozen in liquid nitrogen. X-ray datasets were collected at beamline X29A (National Synchrotron Light Source) using radiation at the Br absorption edge, 0.919 Å (conditions and crystallographic statistics reported in Table S2, which is available at http://jgp.org/cgi/content/full/jgp.200810112/DC1). Data were processed in MOSFLM and scaled in the CCP4 suite. Structures were solved by molecular replacement in PHASER using ion-free wild-type (WT) CLC-F_{AB} complex as a search model (accession no. 1OTS), refined with NCS restraints for the CLC homodimer (but not for the F_{AB}) in REFMAC5 and subsequently in PHENIX, and finally adjusted by hand for stereochemical violations using COOT. Br^- ions, located by anomalous difference maps, were found at the expected Cl^--binding sites. Coordinates and structure factors are deposited in the PDB (3EJY for E203H and 3EJZ for E203V).

Online Supplemental Material

The supplemental material includes three tables. Table S1 reports details of the reaction of thiol reagents with the single-cysteine construct E203C. Table S2 surveys the amino acid frequency at the E203 equivalent position among ∼600 CLC entries in the Uniprot database. Table S3 reports crystallographic statistics for the two x-ray crystal structures determined here. Tables S1–S3 are available at http://www.jgp.org/cgi/content/full/jgp.200810112/DC1.

RESULTS

Our purpose here is to challenge the Glu_{in} position with a variety of mutations and to gauge their effects on Cl^-/H^+

exchange. The proposal that Glu_{in} acts as an essential H^+ shuttle makes a strong prediction: any nonprotonatable residue substituted here should prevent H^+ from participating in the transport cycle; such substitutions might affect the absolute rate of Cl^- transport, but any Cl^- flux remaining should be "uncoupled," i.e., purely passive and unaccompanied by H^+ movement (Walden et al., 2007). Protonatable side chains other than Glu might—or might not—support coupled Cl^-/H^+ exchange, according to this proposal. We therefore assessed the behavior of CLC-ec1 transporters mutated at Glu_{in} via three methods performed with purified protein reconstituted into phospholipid membranes: (1) H^+ pumping driven by Cl^- gradients in liposomes, (2) I-V relations in planar lipid bilayers in the presence of Cl^- or pH gradients, and (3) passive downhill Cl^- turnover rate. Table I reports empirical metrics for these three activities for all mutants tested.

H^+ Pumping

Fig. 1 illustrates proton-pumping traces for all Glu_{in} substitutions. These recordings of the pH of reconstituted liposome suspensions indicate the ability of an outwardly directed Cl^- gradient to drive proton uptake against a pH gradient at zero voltage (Accardi and Miller, 2004; Nguitragool and Miller. 2007). The three side chains supporting robust activity all have protonatable groups (E, D, and H), whereas the basic substitutions (K and R) display slow but unambiguous proton pumping. All mutants lacking protonatable side chains (G, A, S, T, V, I, L, Q, and F) are inactive. Segregation of the side chains into dissociable-active/non-dissociable–inactive categories is not perfect, however, as two of the inactive mutants (C and Y) also carry protonatable side chains. Very low, near-baseline proton uptake appears for several non-dissociable mutants scored as inactive (e.g., G, S, and Q); this may represent real but weak pumping due to direct, inefficient proton donation from solvent hydronium ion, but alternatively, it may be artifactual H^+ movement resulting from small transmembrane imbalances in ionic activity coefficients.

Stoichiometry of Coupled H^+/Cl^- Transport

A quantitative measure of H^+/Cl^- coupling can be derived from electrical recording of transporter-mediated currents. Here, selected CLC variants are inserted into

TABLE I

Transport Metrics for Glu_{in} Mutants

	Turnover rate (s^{-1})	H^+ pumping (nmol/μg protein)	V_r, Cl^- (mV)	V_r, pH (mV)
Coupled transporters				
E (WT)	2,200 ± 200 (3)	23 ± 3 (7)	38.0 ± 0.7 (4)	−58.0 ± 0.4 (4)
D	1,700 ± 90 (4)	22 ± 4 (6)	37.8 ± 0.3 (4)	−57.0 ± 0.6 (4)
H	1,700 ± 50 (4)	22 ± 2 (8)	40 ± 1 (11)	−51± 1 (11)
K	700 ± 30 (4)	7.5 ± 1 (7)	44 ± 2 (6)	−34 ± 1 (6)
R	300 ± 30 (4)	3.8 ± 0.5 (6)	44 ± 1 (3)	−18 ± 1 (3)
Uncoupled transporters				
S	500 ± 30 (4)	2.9 ± 0.5 (5)	51.7 ± 0.8 (10)	
G	330 ± 20 (4)	2.5 ± 0.03 (3)		
T	160 ± 30 (4)	1.7 ± 0.1 (3)		
Q	700 ± 40 (4)	1.5 ± 0.2 (3)		
A	190 ± 10 (4)	1.5 ± 0.1 (5)	53.7 ± 0.9 (5)	0.5 ± 0.2 (5)
C	70 ± 3 (4)	1.3 ± 0.03 (3)	51.0 ± 1.4 (5)	0.3 ± 0.7 (5)
F	210 ± 10 (4)	1.1 ± 0.03 (3)		
Y	140 ± 10 (3)	0.8 ± 0.2 (4)		
L	70 ± 3 (4)	0.4 ± 0.05 (4)		
I	50 ± 2 (4)	0.3 ± 0.03 (3)		
V	40 ± 3 (4)	0.3 ± 0.1 (4)	54.0 ± 2.1 (3)	0.0 ± 0.0 (3)
Non-natural side chains (see Fig. 5)				
E203C/Cys-less		0.3 ± 0.1 (4)		
Cys-1		5.7 ± 0.2 (3)		
Cys-2		1.2 ± 0.1 (4)		
Cys-3		3.3 ± 0.13 (3)		
Cys-4		0.3 ± 0.1 (4)		

Three types of functional assays were quantified as described in Materials and methods on CLC-ec1 transporters with Glu_{in} substituted by the indicated residues. Columns report: (1) Cl^- turnover rate, (2) amplitude of H^+ uptake after 30 s, (3) reversal potential in 10-fold Cl^- gradient, and (4) reversal potential in 3-unit pH gradient. Values represent mean ± SE of the indicated number of separate reconstitutions, in some cases with separate protein preparations. For comparison, values for the uncoupled Glu_{ex} mutant E148A are (Accardi and Miller, 2004; Jayaram et al., 2008): turnover rate: 460 ± 10 s^{-1} ; V_r (H^+): 0 ± 3 mV.

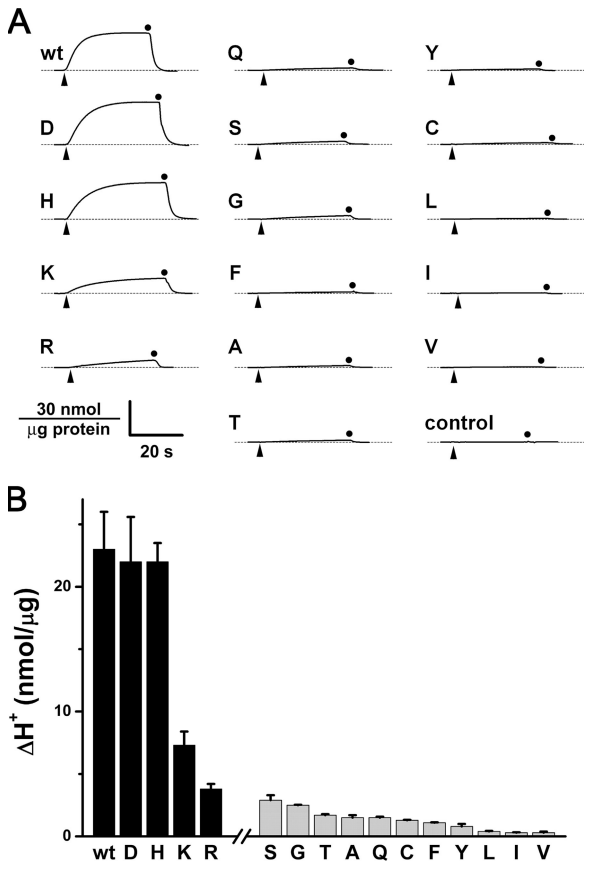

Figure 1. Cl^--driven H^+ pumping in E203 mutants. Uphill movements of H^+ driven by Cl^- gradients were examined in WT CLC-ec1 and the indicated Glu_{in} mutants. (A) Raw recordings of pH of the liposome suspension, with upward deflection indicating proton uptake against a pH gradient. Transport was triggered by the addition of Vln (wedge) and reversed by FCCP (circle). (B) Summary of proton uptake measured after 30 s, with black or gray bars indicating coupled or uncoupled mutants, respectively, as determined from direct coupling measurements (Fig. 2). Each bar represents mean ± SEM of approximately three to eight determinations.

planar bilayer membranes separating solutions with Cl^- or pH gradients (Nernst potentials E_{Cl} and E_H) to which voltage pulses are applied (Fig. 2 A). The reversal potential—the zero-current voltage—is then a direct measure of the H^+/Cl^- transport ratio, r (Accardi and Miller, 2004):

$$V_r = \frac{1}{1+r}\left(E_{Cl} + rE_H\right). \quad (1)$$

Fig. 2 B displays I-V curves representative of well-coupled, poorly coupled, and uncoupled mutants, and reversal potentials are reported in Fig. 2 C for a wider set of mutants. In a 3-unit pH gradient with symmetrical 300 mM Cl^-, the Asp and His mutants show a large negative reversal potential of ∼55 mV, equivalent to r∼0.4–0.5; thus, these mutants maintain the normal two-to-one stoichiometry observed for all CLC exchangers examined quantitatively. The Lys and Arg mutants are only partially coupled, with reversal potentials well below the WT value, as might be anticipated from the weaker H^+ pumping observed for these substitutions (Fig. 1). The uncoupled Val, Ala, and Cys mutants reverse at zero voltage, as expected from their inability to pump protons (Fig. 1). The I-V curve shapes vary somewhat among the mutants, as if the side chains differently influence the unknown steps of the transport cycle. These electrophysiological results are fully consistent with the proton-pumping experiments above.

In a 10-fold Cl^- gradient (symmetrical pH 4.0) the coupled mutants reverse at 35–40 mV, far short of the Cl^- Nernst potential (∼58 mV), a direct indication that H^+ also moves through the protein. The loss of H^+ movement in the uncoupled mutants shifts the I-V curves close to E_{Cl}. These mutations thus preserve the normal anion selectivity of the protein's Cl^- pathway, as with other uncoupling conditions previously documented (Accardi and Miller, 2004; Nguitragool and Miller, 2006; Walden et al., 2007).

Unitary Cl^- Turnover Rates of Glu_{in} Mutants

To investigate effects of the mutations on Cl^- transport, we measured turnover rates under standard "Cl^- dump" conditions at zero voltage: 300 mM Cl^-, pH 4.5, at 25°C, as described in detail (Walden et al., 2007; Jayaram et al., 2008). Liposomes loaded with high KCl were suspended in low Cl^- (but equal K^+), and efflux of KCl was initiated by adding Vln, a K^+-specific ionophore that renders Cl^- movement rate limiting and sets the liposome voltage to zero; a proton ionophore was also present to prevent the buildup of a pH gradient during the Cl^- efflux, and at the end of the time course the total trapped volume was determined by disrupting the liposomes with detergent. Representative traces of Cl^- appearing in the liposome suspension are shown (Fig. 3 A) for representative CLC variants, and unitary turnover rates calculated from these data are reported for all mutants in Fig. 3 B. Cl^- flux correlates with H^+ pumping above; the fastest transporters are the most coupled ones, and all the uncoupled transporters are slower than WT.

In light of the strict conservation of Glu_{in} among the CLC exchangers and of the proposed influence of local electrostatics on anion binding in the Cl^- pathway (Faraldo-Gomez and Roux, 2004), we were surprised that the positively charged substitutions (H, K, and R) all support H^+/Cl^- exchange. Because these residues are so much more basic than Glu, we expected altered pH rate profiles. But the facts contradict this expectation: in the His and Lys mutants, the pH dependence of Cl^- turnover rate is strikingly similar to WT (Fig. 4), despite the huge difference in pK_a values of the amino acid side chains, which span a range of 4 to 12.

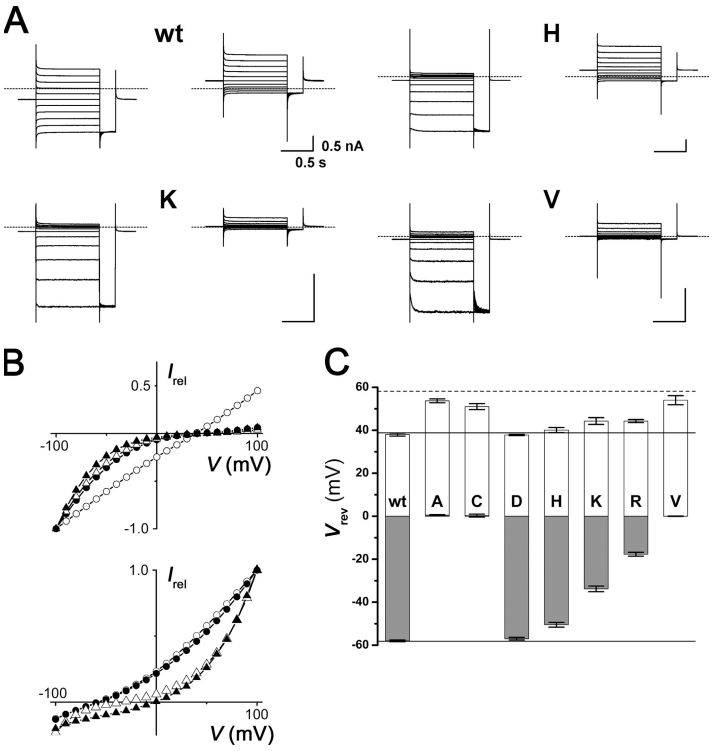

Figure 2. H^+/Cl^- coupling via electrical recording. The indicated CLC transporters in liposomes at high density (50 µg/mg lipid) were incorporated into planar lipid bilayers, and ionic currents were evoked by voltage pulses from −100 to 100 mV in 10-mV increments. (A) Representative current traces, with either 10-fold Cl^- (left of label) or 3-unit pH (right of label) gradients across the bilayer. Dashed lines mark zero-current level. For clarity, currents are displayed in 20-mV increments. All scale bars represent 0.5 nA, 500 ms. (B) I-V curves in either a Cl^- gradient (top) or pH gradient (bottom): open circle, WT; filled circle, H; open triangle, K; filled triangle, V. Currents averaged between 900 and 950 ms into the test pulses are normalized to the values at −100 mV (Cl^- gradient) or +100 mV (pH gradient). (C) Reversal potentials (V_r) were determined by null-point measurement either in Cl^- (open bars) or pH gradient (filled bars). Solid lines indicate theoretically expected values for 1:2 H^+/Cl^- coupling for each type of gradient; dashed line marks Nernst potential (58 mV) for the Cl^- gradient experiment. Each bar represents mean ± SEM of 3–11 measurements.

Effects of Side Chain Chemistry on H^+ Pumping

The Cys mutant above offers opportunities to plant non-natural side chains at Glu_{in} and thereby examine the influence of side chain length and acidity on transporter function. For these experiments, we used a fully functional "Cys-less" transporter with the three natural cysteines in CLC-ec1 replaced by inoffensive residues; Glu_{in} was then substituted on this background with Cys to create a single-Cys mutant that behaves identically to the same substitution on the WT background: slow Cl^- turnover rate and complete loss of H^+ pumping. Reaction of this mutant with iodoacetate or fluoro-iodoacetate introduces carboxyl-bearing side chains one atom unit longer than Glu and of substantially different acidities (Fig. 5 and Table I); the IAA adduct (Cys-1, pK_a ∼4.0) pumps protons at 25% of WT activity, whereas activity of the more acidic fluorinated isostere (Cys-2, pK_a ∼2.0) is further lowered by another factor of 5. Lengthening the side chain by two additional atom units while maintaining the WT acidity (Cys-3, pK_a ∼4.5) reduces pumping activity to 15% of WT; however, a sulfonate-bearing side chain of similar length but far greater acidity (Cys-4, pK_a ∼0) is fully inhibited, as though this side chain is effectively nonprotonatable at the pH of the assay.

Crystal Structures of Coupled and Uncoupled Mutants

X-ray crystal structures were determined at 2.9–3.2 Å resolution for two of the mutants described above (Table S2): one fully coupled and fast (His), the other completely uncoupled and slow (Val). Crystals were grown in Br^-, a functional Cl^- substitute (Nguitragool and Miller, 2006), to allow unequivocal visualization of the bound anion by anomalous diffraction (Lobet and Dutzler, 2005; Accardi et al., 2006). The backbone trajectories of the two mutants are virtually identical to WT (C_α rmsd 0.35, 0.41 Å), as shown in Fig. 6 A, and the structures are also alike in the mechanistic heart of the protein—the ion-coupling region between Glu_{ex} and Glu_{in} (Fig. 6 B). In both mutant structures, as with WT, the dehydrated central Br^- ion is occluded, blocked toward the extracellular side by the deprotonated Glu_{ex} carboxylate, and toward the intracellular by an inner gate formed by S107 and Y445 (Jayaram et al., 2008). Moreover, anion occupancy of the Cl^- pathway is similar to that seen in both WT and the uncoupled Gln substitution (Accardi et al., 2006), with Br^- ions producing prominent anomalous difference peaks in the inner and central sites. We therefore cannot attribute the low Cl^- transport rate in the Val mutant to physical disruption of the Cl^- pathway; instead, we imagine that inhibition of Cl^- flux arises from the unavailability of transportable protons, a circumstance that stalls the transport cycle. The His mutant, being well coupled, does not suffer this disability.

Despite its overall structural similarity, the Val mutant differs from WT in one striking way. In the mutant, electron density is missing, through disorder, for the R28 side chain (Fig. 6 B), which in WT forms a cross-subunit salt bridge with Glu_{in}; disordering of R28 also occurs in the uncoupled Gln mutant (Accardi et al., 2005). In contrast, in the well-coupled His mutant, R28 side chain density appears in precisely the same position as in WT,

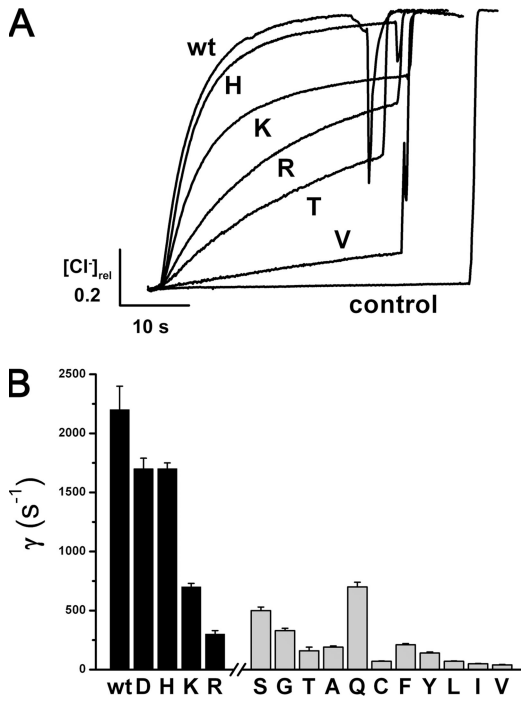

Figure 3. Cl^- efflux rates. (A) Representative "Cl^--dump" traces from the indicated transporters reconstituted at 5 μg/mg lipid, except for "control" trace from protein-free liposomes. Passive Cl^- efflux was triggered by the addition of Vln/FCCP and followed with a Cl^- electrode. Trapped Cl^- was released with 50 mM octylglucoside at the end of the experiment (abrupt upward deflections). Cl^- traces are normalized to the final concentration after the disruption of the liposomes. (B) Unitary turnover rate, γ, plotted in order of proton-pumping activities reported in Fig 1. Each bar represents mean ± SEM of three to four runs.

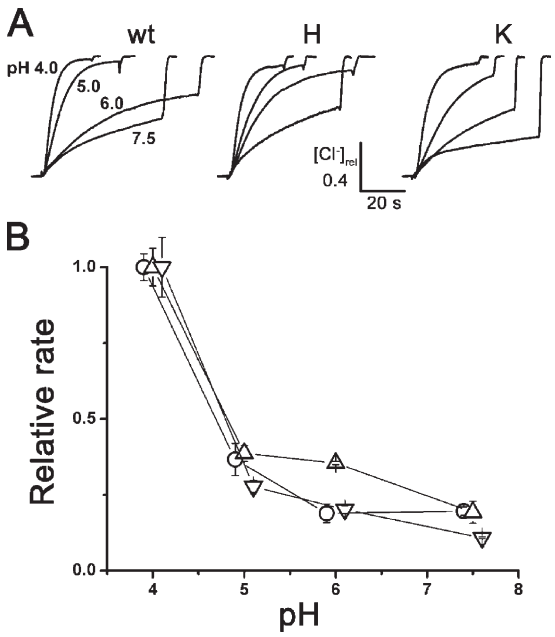

Figure 4. pH dependence of Cl^- flux. Passive Cl^- efflux of coupled transporters was assayed at the indicated pH and maintained symmetrically with citrate-phosphate buffer. (A) Normalized traces of Cl^- efflux, as in Fig 3. (B) Initial rate of Cl^- efflux is normalized to the pH 4.0 value for each transporter: circle, WT; triangle, H; inverted triangle, K.

now with a guanidinium nitrogen within respectable H-bonding distance (3.1 Å) of a His imidazole nitrogen, presumably deprotonated. It is therefore tempting to suppose that an intimate interaction between the proton-transfer group and R28—a salt bridge in WT or a hydrogen bond in the His mutant—is required for an efficient transport cycle; but that idea swiftly collapses (Accardi et al., 2005) with the "negative result" that R28L displays WT-like coupling and Cl^- turnover rate, as we have also confirmed with R28Q and R28E (not depicted).

DISCUSSION

These experiments are simply summarized. Cl^-/H^+ exchange transport in CLC-ec1 occurs only if the Glu_{in} position carries a protonatable group. The chemical nature of the proton-competent side chains is remarkably wide-ranging: WT coupling by carboxyls on Glu, Asp, and by imidazole nitrogen on His, partial coupling by carboxyls of long-chain Cys adducts, by the primary amine of Lys, and even by guanidinium of Arg. Such variety in side chain size, shape, charge, and pK_a is unanticipated for a key mechanistic residue, but it highlights the one feature common to all competent side chains: an ability to bind and release protons, a fundamental requirement for proton transfer. This capability is necessary but not sufficient, as no side chain lacking a dissociable group supports H^+ movement, but several protonatable moieties (thiol, phenol, and sulfonate) fail in this task.

Another pattern emerging here is that the absolute rate of Cl^- transport correlates impressively, although imperfectly, with the degree of H^+ coupling. The fully coupled transporters are fast, 1,000–2,000 s^{-1}, whereas the uncoupled variants move Cl^- at 2–30% of the WT rate. Inhibited turnover in uncoupled exchangers is unsurprising for mechanisms in which protonation is linked to Cl^- binding and conformational change; mutants inept at moving protons through the protein interior could jam the transport cycle and thereby provide Cl^- ions with rare opportunities to slip passively through the protein's anion pathway (Walden et al., 2007; Jayaram et al., 2008). It is particularly intriguing that the Val substitution shows the slowest Cl^- flux of all because this residue appears at the equivalent position in all known channel-type CLC homologues (Accardi et al., 2005). The segregation of CLC channels carrying Val and exchangers carrying Glu is mirrored in the ∼600 CLC sequences in the current Uniprot database, which fall into "Glu" or "Val" subtypes, with infrequent exceptions (Table S3).

These results on a bacterial exchanger are largely harmonious with similar experiments on the equivalent position in two human homologues, CLC-4 and CLC-5

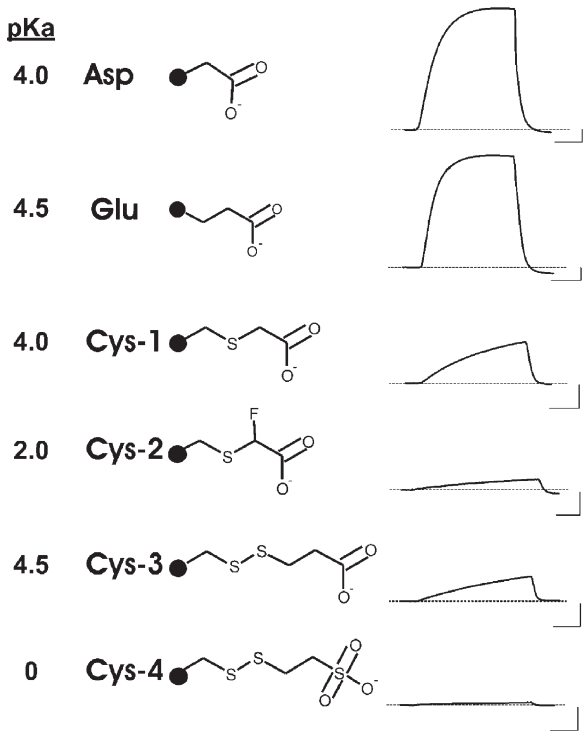

Figure 5. Influence of side chain length and acidity on H^+ transport. Proton pumping (traces on right) was compared for exchangers carrying the side chains indicated. Nominal aqueous pK_a values, reported to ±0.5 unit, are taken from model compounds or calculated in SciFinderScholar software. Non-natural side chains were introduced on Cys-less background by reaction of the E203C mutant with IAA (Cys-1), FIAA (Cys-2), 2-carboxylethyl methanethiosulfonate (Cys-3), or 2-sulfonatoethyl methanethiosulfonate (Cys-4). Reactions were >90% complete for all reagents except FIAA, which reacted to only 70% completion; any unmodified Cys mutant, being inactive (Fig. 1), does not contribute to the signal. Scale bars represent 4 nmol/μg protein, 10 s.

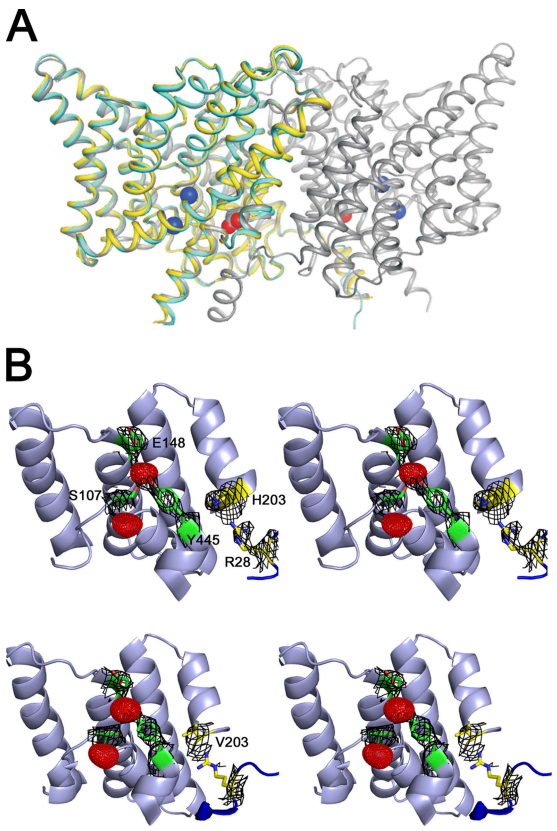

Figure 6. X-ray crystal structures of CLC-ec1. CLC-ec1 mutants E203H (PDB accession no. 3EJY) and E203V (3EJZ) were crystallized with Br^- substituting for Cl^- in all solutions. Structures are displayed with the extracellular side facing upward. (A) Structural alignment of CLC variants. Backbone trace of homodimeric WT protein is shown in gray, with single subunits of E203H (yellow) and E203V (cyan) superimposed by alignment of residues 20–200. Blue spheres represent Cl^- ions, and Glu_{in} is indicated by space-filled atoms in the WT. (B) Stereo views of ion-coupling region between Glu_{in} and Glu_{ex} positions. Br^- ions appear as anomalous difference maps (red) contoured at 5σ. $2F_o$–F_c electron density maps (black) are shown near the Glu_{in} position, including R28, contoured at 0.8–1 σ. Outer gate (Glu_{ex}) and inner gate (S107/Y445) are shown in green sticks. Part of the N-terminal helix from the twin subunit carrying R28 is shown in blue; Val and His substitutions at Glu_{in} and R28 are rendered in yellow/blue sticks.

(Zdebik et al., 2008). In that study, Cl^- /H^+ antiport occurred with E, D, H, or Y at the Glu_{in} position, but not with A, R, V, C, M, and N; moreover, mutants failing in H^+ transport also failed in Cl^- transport. With CLC-ec1, however, we observe Cl^- transport in all H^+-uncoupled mutants, albeit at lowered rates. This apparent discrepancy between the bacterial and eukaryotic CLCs is not serious because the CLC-4/CLC-5 experiments used voltage clamp recording in *Xenopus* oocytes, which might miss slow, uncoupled Cl^- transport buried in the background "leak" currents intrinsic to the recording system. However, the H^+ transport activity seen in the Tyr mutant of the human CLCs appears to be a real difference between the homologues, as the liposome assay used here would have picked up comparable proton-pumping activity.

This survey of proton transfer on the intracellular side of CLC-ec1 expands previous work (Accardi et al., 2005; Zdebik et al., 2008) and buttresses the idea that the carboxyl group of Glu_{in} does indeed act as a H^+ shuttle essential for coupling ion movements in CLC exchangers. However, the details of the H^+ transfer step itself remain vague. A central issue, conspicuous by our ignorance about it, is the pathway taken by the proton after it leaves Glu_{in} on its way to Glu_{ex} ~15 Å away. We previously argued (Accardi et al., 2006) that the central Cl^- ion itself, located halfway between these two glutamates, acts as a critical way station in the proton pathway. But this still leaves ~8 Å of nominally nonpolar distance that the proton must traverse to reach that site. A recent molecular dynamics study (Voth, G., personal communication) observes that upon protonation in silico, Glu_{in} rotates toward the central Cl^- as several intracellular water molecules enter to mediate the required H^+ transfer. Although experimental work is currently silent on whether such a side chain rearrangement actually occurs in proteo, a mechanism like this

would neatly account for proton transfer on the intracellular side of CLC exchangers.

It is also worthwhile to puzzle over the pH dependence of Cl^- turnover, which is unexpectedly insensitive to the pK_a of the intracellular H^+ transfer residue. Previous work showed that Cl^- flux varies with pH in response to titration of the extracellular proton-transfer gate (Accardi et al., 2004, 2005). We infer from this that ion transport is rate limited by the extracellular H^+ transfer step (which is linked to conformational rearrangement of Glu_{ex}), and that intracellular H^+ transfer must be much faster than this. Only when intracellular H^+ transfer is severely compromised, as by the nonprotonatable or highly acidic/basic side chains described here, does its influence on Cl^- transport become apparent.

The results set the stage for attacking future questions about how protons move between solvent and Glu_{in}. This is not a trivial process. In crystal structures, the side chain at this position, although physically close to solvent, is not directly exposed to it. Rather, it is covered by the N-terminal helix from the twin subunit in the homodimer. If this helix were sufficiently mobile, direct protonation of Glu_{in} from solvent could occur; alternatively, solvent protons might first bind to carboxylates located nearby on the water-exposed surface, as in the "proton antennas" that accelerate proton-transfer steps above the formal diffusion limit in membrane proteins, such as photosynthetic reaction centers or cytochrome c oxidase (Ädelroth and Brzezinski, 2004; Bränden et al., 2006). Experimental evidence on CLC exchangers is still too primitive to address possibilities like this. In any case, because the H^+ transport rate of CLC-ec1, $\sim$1,000 s^{-1} at pH 4.5, is approximately three orders of magnitude below the diffusion limit, no special mechanisms need be invoked for the protein to achieve its biological purpose: facilitating extreme acid resistance in *E. coli* (Iyer et al., 2002).

We thank the X29A beamline staff at the National Synchrotron Light Source, Brookhaven National Laboratories, where crystallographic data collection was supported by the U.S. Department of Energy (contract no. DE-AC02-98CH10886). We are grateful to Dr. Greg Voth for informing us of molecular dynamics results before publication, and to Dr. Hari Jayaram for compiling statistics for Table S3, for unceasing crystallographic advice, and for invaluable ridicule/humiliation on drafts of the manuscript.

This work is supported in part by National Institutes of Health (grant RO1-31768).

Edward N. Pugh Jr. served as editor.

Submitted: 26 August 2008
Accepted: 18 December 2008

REFERENCES

Accardi, A., and C. Miller. 2004. Secondary active transport mediated by a prokaryotic homologue of ClC Cl^- channels. *Nature.* 427: 803–807.

Accardi, A., L. Kolmakova-Partensky, C. Williams, and C. Miller. 2004. Ionic currents mediated by a prokaryotic homologue of CLC Cl^- channels. *J. Gen. Physiol.* 123:109–119.

Accardi, A., M. Walden, W. Nguitragool, H. Jayaram, C. Williams, and C. Miller. 2005. Separate ion pathways in a Cl^-/H^+ exchanger. *J. Gen. Physiol.* 126:563–570.

Accardi, A., S. Lobet, C. Williams, C. Miller, and R. Dutzler. 2006. Synergism between halide binding and proton transport in a CLC-type exchanger. *J. Mol. Biol.* 362:691–699.

Ädelroth, P., and P. Brzezinski. 2004. Surface-mediated proton-transfer reactions in membrane-bound proteins. *Biochim. Biophys. Acta.* 1655:102–115.

Bränden, G., R.B. Gennis, and P. Brzezinski. 2006. Transmembrane proton translocation by cytochrome c oxidase. *Biochim. Biophys. Acta.* 1757:1052–1063.

DeAngeli, A., D. Monachello, G. Ephritikhine, J.M. Frachisse, S. Thomine, F. Gambale, and H. Barbier-Brygoo. 2006. AtCLCa, a proton/nitrate antiporter, mediates nitrate accumulation in plant vacuoles. *Nature.* 442:939–942.

Dutzler, R., E.B. Campbell, and R. MacKinnon. 2003. Gating the selectivity filter in ClC chloride channels. *Science.* 300:108–112.

Faraldo-Gomez, J.D., and B. Roux. 2004. Electrostatics of ion stabilization in a ClC chloride channel homologue from Escherichia coli. *J. Mol. Biol.* 339:981–1000.

Graves, A.R., P.K. Curran, and J.A. Mindell. 2008. The Cl^-/H^+ antiporter CLC-7 is the primary chloride permeation pathway in lysosomes. *Nature.* 453:788–792.

Iyer, R., T.M. Iverson, A. Accardi, and C. Miller. 2002. A biological role for prokaryotic ClC chloride channels. *Nature.* 419:715–718.

Jayaram, H., A. Accardi, F. Wu, C. Williams, and C. Miller. 2008. Ion permeation through a Cl^--selective channel designed from a CLC Cl^-/H^+ exchanger. *Proc. Natl. Acad. Sci. USA.* 105:11194–11199.

Jentsch, T.J. 2008. CLC chloride channels and transporters: from genes to protein structure, pathology and physiology. *Crit. Revs. Biochem. Mol. Biol.* 43:3–36.

Lobet, S., and R. Dutzler. 2005. Ion binding properties of the CLC chloride selectivity filter. *EMBO J.* 25:24–33.

Miller, C. 2006. ClC chloride channels viewed through a transporter lens. *Nature.* 440:484–489.

Miller, C., and W. Nguitragool. 2009. A provisional transport mechanism for a CLC-type Cl^-/H^+ exchanger. *Philos. Trans. R. Soc. Lond. B. Biol. Sci.* 364:175–180.

Nguitragool, W., and C. Miller. 2006. Uncoupling of a CLC Cl^-/H^+ exchange transporter by polyatomic anions. *J. Mol. Biol.* 362: 682–690.

Nguitragool, W., and C. Miller. 2007. CLC Cl^-/H^+ transporters constrained by covalent cross-linking. *Proc. Natl. Acad. Sci. USA.* 104:20659–20665.

Picollo, A., and M. Pusch. 2005. Chloride/proton antiporter activity of mammalian CLC proteins ClC-4 and ClC-5. *Nature.* 436:420–423.

Scheel, O., A.A. Zdebik, S. Lourdel, and T.J. Jentsch. 2005. Voltage-dependent electrogenic chloride/proton exchange by endosomal CLC proteins. *Nature.* 436:424–427.

Walden, M., A. Accardi, F. Wu, C. Xu, C. Williams, and C. Miller. 2007. Uncoupling and turnover in a Cl^-/H^+ exchange transporter. *J. Gen. Physiol.* 129:317–329.

Zdebik, A.A., G. Zifarelli, E.Y. Bergsdorf, P. Soliani, O. Scheel, T.J. Jentsch, and M. Pusch. 2008. Determinants of anion-proton coupling in mammalian endosomal CLC proteins. *J. Biol. Chem.* 283: 4219–4227.

Zifarelli, G., and M. Pusch. 2007. CLC chloride channels and transporters: a biophysical and physiological perspective. *Rev. Physiol. Biochem. Pharmacol.* 158:23–76.